

**Author version:** *Mar. Pollut. Bull.*, vol.114(2); 2017; 805-815

## **Offshore sediments record the history of onshore iron ore mining in Goa State, India**

Tyson Sebastian<sup>1\*</sup>, B.Nagender Nath<sup>1</sup>, Sangeeta Naik<sup>1</sup>, D.V.Borole<sup>1</sup>, Salou Pierre<sup>2</sup>, Armoury Kazip Yazing<sup>1</sup>

<sup>1</sup> CSIR-National Institute of Oceanography, Dona Paula, Goa-403 004

<sup>2</sup> ENSIL - Ecole Nationale Supérieure d'Ingénieurs de Limoges, University of Limoges, France

Corresponding author email: tsebastian@nio.org

### **Abstract**

Environmental magnetic and geochemical analyses combined with <sup>210</sup>Pb dating were carried out on a sediment core off Goa from Arabian Sea to reconstruct the sedimentation history of last three and a half centuries and to investigate the impact of onshore iron ore mining on the offshore sedimentation. A drastic increase in sedimentation rate and mineral magnetic concentration parameters divides the core into two units (1 & 2) at a depth of 41 cm (1982 AD). The high magnetic susceptibility values in Unit 1 sediments are coeval with increased iron ore production on land and illustrate the role of terrestrial mining on the increased offshore sedimentation. The early diagenetic signals were observed in Unit 2 of the core with low concentration parameters, coarse magnetic grain size and magnetically hard mineralogy. The geochemical data of the core also record the Little Ice Age (LIA) climatic events of Dalton and Maunder solar minima.

**Keywords:** Environmental magnetism, Iron ore mining, Sedimentation rate, <sup>210</sup>Pb dating, Anthropogenesis

## **Introduction**

Iron and manganese mining in Goa, a coastal state of India, is carried out by open cast method which necessitates the removal of surface material overlying the ore formations. The total land area covered by these mines is approximately 30,325 ha, which is about 8% of the total geographical area of the state ([www.cseindia.org/node/386](http://www.cseindia.org/node/386)). There were 334 mining leases in existence out of which 82 were in operation during the period 2009-10 ([www.goadm.gov.in/MiningArea.aspx](http://www.goadm.gov.in/MiningArea.aspx)). The average annual iron ore production in Goa was about 28 million tonnes (Mt) during the years 2002 – 2011 and the mining waste generated during this period was thrice the amount of production. The two major rivers in Goa, Mandovi and Zuari flow through the mining belt (**Fig. 1**) and bring the mining wastes as dissolved and particulate load to the Mandovi – Zuari estuarine system. The transport of ore in barges through the waters of Mandovi and Zuari estuarine system to the Mormugoa Port for export also generates a lot of waste adding up to the water – and wind – borne mining waste.

The environmental impact of Goan iron ore mining is discussed in various publications. The effect of mining on foraminiferal abundance (Nigam et al., 2005), trace metal concentration (Alagarsamy, 2006; Fernandes and Nayak, 2009; Mesquita and Kaisary, 2007; Zingde et al., 1976), rare earth element geochemistry (Shynu et al., 2013, 2011), and magnetic properties (Kessarkar et al., 2015; Prajith et al., 2015; Singh et al., 2014) were mainly assessed in the Mandovi – Zuari estuarine system and the impact of the mining on the coastal environment is poorly known. A biomarker study (Kurian et al., 2009) of a 700 year sediment record of primary productivity from the inner shelf of Goa (14.98°N, 74°E, water depth ~ 45 m) has showed large shifts during the last ~ 50 years which has been attributed to indicate the greatly enhanced productivity in response to high solar irradiance as well as anthropogenic input of nutrients. Whether these shifts during the last 50 years are related to the increased iron ore production since 1950s is not known. Here, an attempt is made to reconstruct the history of sedimentation in the inner shelf of Goa using mineral magnetic and geochemical techniques and to assess if the offshore sediments are affected by mining-related activities on land.

## **Materials and Methods**

### **1. Study area and sampling**

Goa State in India lies within the geographical coordinates located between 14.90° - 15.80°N and 73.68° - 74.33°E covering an area of 3,701 sq. km. Geologically, it is a part of the Dharwar Craton of the South Indian Shield and is covered mostly by the metamorphic rocks of Archean – Proterozoic age. The Deccan Traps of Late Cretaceous to Eocene are exposed in a small area along the NE

border of Goa. In most of the areas these rocks are covered by a thick layer of laterite and aluminous–laterite of Pliocene to Pleistocene time (Gokul et al., 1985). The climate of Goa is humid tropical with an annual average rainfall of 300–350 cm of which a major portion is received during the south-west monsoon.

The 1.03 m long gravity core (named as SASU 177 - GC 5) investigated in this study was collected from Arabian Sea off Goa at 15.50°N; 73.65°E, during the 177<sup>th</sup> cruise of RV Sagar Sukthi in May 2008 (**Fig. 1**). It was collected from a water depth of 24.6 m. The top 100 cm of the core was sub-sampled at 1 cm interval. The sediment samples were sealed in plastic bags immediately after sectioning and were stored.

## 2. Chronological Framework

The chronology and the sedimentation rate of the sediment core were established using <sup>210</sup>Pb dating method (Koide et al., 1972; Krishnaswami and Lal, 1978). The short half life of 22.3 years of <sup>210</sup>Pb makes it ideal for estimating recent sedimentation rates. <sup>210</sup>Pb activities of the sediment core were analyzed indirectly by measuring the activity of its granddaughter <sup>210</sup>Po (half life=138.4 d) which is in radioactive equilibrium with <sup>210</sup>Pb (half life=22.3 yr) using isotope dilution alpha-spectroscopy (Flynn, 1968). Briefly, 2 -3 g of powdered sediment sample was digested in presence <sup>209</sup>Po tracer by successive acid treatments and final solution was brought in 0.5N HCl. From this solution, Po isotopes were auto deposited on silver planchets. The alpha activity of Po isotope source was assayed using the EG&G ORTEC ion implanted detector coupled to a multi channel analyzer. The activity of <sup>210</sup>Pb<sub>excess</sub> was estimated from the relation:  $^{210}\text{Pb}_{\text{excess}} = ^{210}\text{Pb}_{\text{total}} - ^{210}\text{Pb}_{\text{supported}}$  where <sup>210</sup>Pb<sub>total</sub> is the total <sup>210</sup>Pb activity measured in the sample and <sup>210</sup>Pb<sub>supported</sub> is the <sup>210</sup>Pb activity which is assumed to be in equilibrium with the parent nuclide. In the present case, the average value of <sup>210</sup>Pb (0.37 dpm/g) in the lowermost section from 55 – 101 cm is taken as the parent supported value. The <sup>210</sup>Pb<sub>excess</sub> value was computed by subtracting this value (0.37 dpm/g) from total <sup>210</sup>Pb activity.

## 3. Environmental Magnetic Measurements

Magnetic susceptibility ( $\chi$ ) of the samples was determined on dried samples using a Bartington MS-2 magnetic susceptibility meter and a MS2B dual frequency sensor. The samples were oven dried at 40°C and gently crushed before packing it into the 10 ml plastic vials. Magnetic susceptibility was measured at both low frequency (0.47 kHz) and high frequency (4.7 kHz) ( $\chi_{\text{LF}}$  &  $\chi_{\text{HF}}$  respectively) and the frequency dependent susceptibility ( $\chi_{\text{FD}}$ ) was determined from the expression  $\chi_{\text{FD}} \% = [(\chi_{\text{LF}} - \chi_{\text{HF}}) / \chi_{\text{LF}}] \times 100$  (Mullins and Tite, 1973).

Anhyseretic remanent magnetization (ARM) is imparted to the sample by the combined effects of a large alternating field (AF) and a small constant DC field. This is done by slowly reducing a peak AF to zero while at the same time applying a constant DC field to the sample (Moskowitz, 1991). In this study, ARM was measured using a Molspin AF demagnetizer and Molspin Spinner magnetometer in a 0.05 mT bias field and a 100 mT peak alternating field. The obtained ARM value was then divided by the weight of the sample in order to get the susceptibility of ARM ( $\chi_{ARM}$ ) which is a grain size dependent parameter. Saturation Isothermal Remnant Magnetization (SIRM) was imparted using a pulsed field of 1T using a Molspin pulse magnetizer. After the acquisition of SIRM, backfields of 20mT, 40mT, 100mT, 300mT were applied. Soft IRM and Hard IRM was calculated from these values using the expressions

$$\text{Soft IRM} = \text{SIRM} - \text{IRM}_{20\text{mT}}$$

$$\text{Hard IRM} = \text{SIRM} - \text{IRM}_{300\text{mT}}$$

The quality of the magnetic measurements was ensured with a Bartington reference material, which was run after every five measurements.

#### **4. Determination of Organic & Inorganic Carbon**

The readily oxidizable organic carbon content was determined by the Walkley-Black method (Walkley, 1947) adopted and modified by (Jackson, 1958). The dried sediment samples were oxidized with  $\text{K}_2\text{Cr}_2\text{O}_7$  and  $\text{H}_2\text{SO}_4$  in the presence of  $\text{Ag}_2\text{SO}_4$ . It was then back titrated with 0.5N ferrous ammonium sulphate solution to a one drop end point after adding  $\text{H}_3\text{PO}_4$ , NaF and diphenylamine indicator.  $\text{CO}_2$  Coulometer was used for the determination of total inorganic carbon (TIC). The accuracy of the measurements was ensured with a Calcium Carbonate standard.

#### **4. Major and trace element analyses**

The major and trace element concentrations in the core were measured using ICP – MS and AAS. The powdered sediment samples were digested using a 7:3:1 acid mixture ( $\text{HF}:\text{HNO}_3:\text{HClO}_4$ ) in Teflon beakers. After the digestion, the solution was filtered and analysed using ICP – MS (Inductively Coupled Plasma Mass Spectrometer Thermo Scientific, XSERIES 2, Quadrupole) at CSIR - NIO. The Fe content in the sediments was measured using AAS (Atomic Absorption Spectrophotometer – Thermo Scientific S Series). The USGS standards W-2 and MAG – 1 were used to ensure the quality of the results. The repeatability of the analyses for Fe was better than  $\pm 5\%$ .

## Results

### Estimation of Sedimentation Rate

The  $^{210}\text{Pb}_{\text{excess}}$  depth profile is shown in Figure 2. The sedimentation rates were estimated from this profile following the Constant Initial Concentration (CIC) model (Koide et al., 1972; Krishnaswami and Lal, 1978). In this method, it is assumed that sediments are having a constant initial excess  $^{210}\text{Pb}$  concentration and the decrease of  $^{210}\text{Pb}_{\text{excess}}$  activity with depth is solely due to radioactive decay. The  $^{210}\text{Pb}_{\text{excess}}$  activity decay with depth shows mainly two trends, first between 0 and 41 cm and the second one between 41 and 51 cm. The sedimentation rate in the top 41 cm of the core was estimated to be 1.57 cm/yr and corresponds to depositional years between 1982 and 2008 AD (year of collection). The sediments between 41 and 51 cm of the core have a lower sedimentation rate of 0.19 cm/yr (**Fig. 2**) and the corresponding calendar age for this section is 1982 – 1929 AD. Dating the remaining part of the core was not possible with the  $^{210}\text{Pb}$  method due to its short half life. From the age - depth model, if it is assumed that sedimentation rate in the area before 1929 AD would have been similar to the second unit with slower sedimentation rate, time span covered by the core (on this assumption) could be ~348 yrs (2008 – 1660 AD). In a previous study, a sediment core off Goa (14.98° N, 74° E, Water depth ~ 45 m) has yielded a closer sedimentation rate (0.15 cm/yr; Kurian et al., 2009 – **Fig. 2**). The two units 0 – 41 cm and 41 – 103 cm, with two different sedimentation rates are hereafter referred as Unit 1 and Unit 2 respectively.

### CaCO<sub>3</sub> and C<sub>organic</sub> variation

CaCO<sub>3</sub> values vary from 3.0% - 39.4% and organic carbon (C<sub>org</sub>) values vary from 2.0 – 3.1 % in the core (**Fig. 3**). The CaCO<sub>3</sub> values are low and nearly constant down up to 95 cm of the core, thereafter showing a distinct increase to ~40. C<sub>org</sub> on the other hand vary narrowly between 2 – 3%.

### Environmental Magnetic Parameters

The major environmental magnetic parameters are classified based on their dependence on the magnetic mineral concentration, grain size and mineralogy.

#### 1) Concentration Parameters

The low and high frequency susceptibilities ( $\chi_{\text{LF}}$ ,  $\chi_{\text{HF}}$ ), Susceptibility of Anhyseric Remanent Magnetization ( $\chi_{\text{ARM}}$ ), Saturated Isothermal Remanent Magnetization (SIRM) are proportional to the concentration of magnetic minerals present in the sample (Thompson and Oldfield, 1986). The downcore profiles of these concentration-dependent magnetic parameters reveal low values in the

Unit 2 and intermediate to high values in the Unit 1 with a gradual increase from 41 cm towards the top of the core (**Fig. 3**). The average values of  $\chi_{LF}$ ,  $\chi_{ARM}$ , SIRM of Unit 1 are  $79.1 \times 10^{-8} \text{ m}^3\text{Kg}^{-1}$ ,  $0.89 \times 10^{-5} \text{ m}^3\text{Kg}^{-1}$  and  $1249.6 \times 10^{-5} \text{ Am}^2\text{Kg}^{-1}$  respectively. In Unit 2, the average values of these parameters are  $19.4 \times 10^{-8} \text{ m}^3\text{Kg}^{-1}$ ,  $0.05 \times 10^{-5} \text{ m}^3\text{Kg}^{-1}$ , and  $205.8 \times 10^{-5} \text{ Am}^2\text{Kg}^{-1}$  respectively. Slightly increased values of  $\chi_{LF}$ ,  $\chi_{ARM}$  and SIRM ( $24.7 \times 10^{-8} \text{ m}^3\text{Kg}^{-1}$ ,  $0.05 \times 10^{-5} \text{ m}^3\text{Kg}^{-1}$  and  $278.5 \times 10^{-5} \text{ Am}^2\text{Kg}^{-1}$  respectively) are observed in the depth range of 83 – 90 cm.

## 2) Grain Size Parameters

ARM is a measure of the concentration of magnetic minerals of stable single domain size range (Oldfield, 1991; Thompson and Oldfield, 1986). The ratios of  $\chi_{ARM} / \chi_{LF}$ ,  $\chi_{ARM}/\text{SIRM}$ , and  $\text{SIRM}/\chi_{LF}$  are also indicators of the grain size of magnetic minerals. The higher values of  $\chi_{ARM} / \chi_{LF}$ ,  $\chi_{ARM}/\text{SIRM}$  indicate a fine magnetic grain size while a higher value of  $\text{SIRM}/\chi_{LF}$  indicates a coarse grain size (Oldfield, 1991; Thompson and Oldfield, 1986; Walden, 1999).  $\chi_{ARM} / \chi_{LF}$  and  $\chi_{ARM}/\text{SIRM}$  ratios show higher values in the Unit 1 of the core indicating a finer grain size. High  $\text{SIRM}/\text{ARM}$  ratios ( $>100$ ) indicate the dominance of multi domain grains and the low ratios ( $<30$ ) indicate dominance of stable single domain grain size (Yu and Oldfield, 1993). The average  $\text{SIRM}/\text{ARM}$  ratio for the top 41 cm of the core is 35 while for the remaining part of the core it is 104. Similarly  $\chi_{ARM} / \chi_{LF}$  and  $\chi_{ARM}/\text{SIRM}$  ratios have values 11.4 and  $73.2 \times 10^{-5} \text{ mA}^{-1}$  in the Unit 1 of the core and 2.6 and  $24.9 \times 10^{-5} \text{ mA}^{-1}$  in the Unit 2 respectively.

The biplot of  $\chi_{fd} \%$  vs.  $\chi_{ARM}/\text{SIRM}$  (**Fig. 4**) is an indicator of the magnetic grain size and the concentration of super paramagnetic (SP) grains (Dearing et al., 1997; Maher, 1998). The sediments representing Unit 1 are scattered in the ‘coarse stable single domain (SSD)’ and ‘Fine SSD & mixtures’ range and the contribution from SP grains is below 50%. The samples from Unit 2 plot on the boundary between ‘multi-domain & pseudo single domain (MD & PSD)’ and ‘coarse SSD’ with varying contribution from SP grains. All these parameters point to the fact that the magnetic grain size coarsens down core and the Unit 1 of the core is composed of mainly Stable Single Domain (SSD) grains while the Unit 2 is composed of coarse SSD or MD grains.

## 3) Mineralogy of Magnetic Minerals

IRM is a function of the magnetic mineralogy and grain size (Oldfield et al., 1999). Hard isothermal remanent magnetization (HIRM) is an indicator of concentration of remanence carrying imperfect antiferromagnets such as hematite and goethite while soft isothermal remanent magnetization (Soft IRM) can be used to approximate the concentration of remanence carrying ferrimagnets such as

Magnetite ((Dekkers, 2007). In these samples the ratio between soft and hard IRM values for the Units 1 and 2 are 8.87 and 5.54 respectively. The decrease in Soft IRM/ HIRM ratio indicates an increase in hematite concentration in the bottom section of the core. S-Ratio can also be used as a parameter to study the relative concentration of magnetite and hematite in the sample. S - ratio values close to unity represent a magnetite only mineralogy while a lower S - ratio corresponds to the presence of hematite. The top 41 cm (Unit 1) of the core shows an S- ratio of 0.90 (relatively higher magnetite content) and the Unit 2 shows a decrease (0.85) indicating relatively higher hematite concentration.

### **Major and Trace elements**

The Fe concentration in the sediment core varied from 3.38% to 8.00% and the Mn concentration ranged between 310 ppm – 921 ppm (**fig. 9**). Fe showed slightly higher values in Unit 1 (6.77%) compared to Unit 2 (6.09%) while the concentration of Mn in Unit 1 (779ppm) was quite high compared to Unit 2 (489 ppm) sediments. The maximum concentration of Fe was at 74 cm depth while for Mn, the maximum values were seen at 10 cm depth.

### **Discussion**

The coeval increase in sedimentation rate and mineral magnetic parameters divide the core into two sections at a depth of 41 cm corresponding to an age of 1982 AD (**Fig.3**). The higher sedimentation rate (1.57 cm/yr) in the Unit 1 indicates that the inner shelf region off Goa is acting as a depocentre of sediment accumulation in recent years. This is extremely consistent with a record from the mudflat region of Mandovi River (one of the two rivers contributing sediments to the continental shelf) where a higher sedimentation rate of 1.42 cm/yr in the top 35 cm (roughly corresponds to year 1980AD) is reported with a slower sedimentation rate (0.14 cm/yr) in the bottom section of their record (Singh et al., 2014) (**Fig. 2**). Lower sedimentation rate (0.19 cm/yr) in the Unit 2 of our study is also comparable to the published value on a sediment core from the continental shelf off Goa from a slightly deeper region (**Fig. 2** - 45m water depth, sedimentation rate 0.15 cm/yr, Kurian et al., 2009).

The increase in sedimentation rate and magnetic mineral concentration in the Unit 1 of the core is possibly due to the extensive open cast iron ore mining in Goa, which covers almost eight percent of its total geographical area. Though the mining in Goa started well before its independence in 1961 from Portugal, it gained its momentum by 1970s and increased thereafter. Iron ore production in Goa has increased from 1.09 Mt in 1953 to 30.7 Mt in 2007 (Nayak, 2002; Pascual et al., 2013). The open cast mining produces a lot of rejects which are transported by wind or water to the estuary and

then possibly to the offshore areas. The transportation of the ores and pellets by mechanised barges along Mandovi and Zuari estuaries to Mormugao Harbour for export, also contribute significant amount of material to the river and estuarine system. An increase in suspended particulate matter (SPM) content in the Mandovi estuary with time after 1980 has been attributed (Nayak, 1998; Nigam et al., 2005; Shynu et al., 2012) to the increased supply of mining induced sediments to the coastal regions of Goa. Mining was mainly concentrated in South Goa region in the initial stages (Sanguem and Quepem administrative units known as talukas locally) where manganese ore was abundant. As the demand for Mn ore diminished, the mining sites shifted from south Goa to iron ore deposits of north Goa (Bicholim taluka) (Panchang et al., 2005 and the references therein). The reason for the very sharp rise in linear sedimentation rate (0.19 to 1.57 cm/yr) at 1982 may be due to this shifting of mining sites to the catchment area of Mandovi River. The increase in mineral magnetic properties after 1980s is also evident from the published record of a mudflat sediment core from Mandovi River (Singh et al., 2014). The comparison between the sedimentation rates and magnetic properties of present study from the offshore region with the results from estuary (Singh et al., 2014) confirms the acceleration of mining activity post 1980 in this region (**Fig. 5**).

A plot of decadal variation in the production of iron ore in Goa during 1950 – 2008 (**Fig. 6**; Nayak, 2002; Pascual et al., 2013) along with the changes in magnetic susceptibility illustrates the manifold increase in the mining in Goa and its impact on the offshore region during the last five decades. This increase was also accompanied by an increase in the sedimentation rate and magnetic mineral concentration as indicated by the increased values of  $\chi_{LF}$  and Fe concentration in the top section of the core. The influence of mining on the magnetic mineral concentration is clearly visible from the synchronous increase of  $\chi_{LF}$  and iron ore production.

A scatter plot of iron content versus magnetic susceptibility (**Fig. 7a**) shows that the Unit 1 is characterized by high susceptibility and high Fe content whereas Unit 2 shows low susceptibility but medium to high Fe content. Although a rapid change in Fe concentration is not observed between the two units, a gradual increase in Fe concentration is visible towards the surface. In Mandovi estuary too, a gradual increase in Fe content towards the top in cores was reported before (Veerasingam et al., 2015). A gradual reduction in Fe content in sediments was reported (Prajith et al., 2015) with high values in the upper (24.8%) reducing in middle (18.0%) with a further reduction in the lower estuary (5.4%). A drastic decrease in the susceptibility from a mean value of  $617 \times 10^{-8} \text{ m}^3\text{kg}^{-1}$  in upper estuary to  $121.7 \times 10^{-8} \text{ m}^3\text{kg}^{-1}$  in lower estuary was reported before (Prajith et al., 2015). Further  $\chi_{LF}$  values were found (Kessarkar et al., 2015) to decrease from upper estuary to the offshore area. Magnetic susceptibility values of Unit 1 are comparable to the previously published values of



shelf sediments (Kessarkar et al., 2015) in the vicinity of our core. **Table 1** compiles the values of major mineral magnetic parameters obtained from different studies in the Mandovi – Zuari estuaries and the offshore region. The present study, when compared with the published values, imply that only a portion of the anthropogenic material is reaching the offshore area while a major portion of it is being deposited in the estuary itself.

The bivariate plots of  $\chi_{\text{ARM}}$  versus  $\chi_{\text{LF}}$  (King's plot) and  $\chi_{\text{ARM}}/\text{SIRM}$  versus  $\chi_{\text{LF}}$  (**Fig. 7c, 7d**) can be used to decipher the concentration and grain size of magnetic minerals (Blaha et al., 2011; King et al., 1982). The higher values of  $\chi_{\text{ARM}}$ ,  $\chi_{\text{LF}}$  and  $\chi_{\text{ARM}}/\text{SIRM}$  in Unit 1 (In **Fig. 7c and 7d**) indicate the presence of high concentration of magnetic minerals which are fine grained in nature. Sediments in unit 2 are relatively depleted in magnetic minerals and are magnetically coarse grained. Magnetite, hematite and goethite are the predominant minerals in the iron ore deposits of Goa (Prajith et al., 2015). The increase in S ratio and Soft IRM/ HIRM values towards core top suggest an increase in the concentration of fine grained magnetite and a decrease in antiferromagnetic minerals in Unit 1. In contrast, coarse grained antiferromagnetic minerals are high in unit 2. The biplot of S - ratio and  $\chi_{\text{LF}}$  (**Fig. 7b**) illustrates this change and separates the mining influenced sediments from the natural background signals.

The magnetic susceptibility ( $\chi_{\text{LF}}$ ) values were also compared with the Konkan – Goa rainfall for the years (1980 – 2008) to study the influence of rainfall related runoff if any (**Fig. 8**). The comparison is only made for the period with high sedimentation rate. The graph shows similar trends indicating that the deposition of magnetic minerals was primarily associated with rainfall. The low rainfall years were marked with low values of magnetic susceptibility while the strong monsoon years resulted in increased susceptibility. The enhanced monsoonal precipitation in the catchment area may have facilitated increased runoff from rivers and thereby increasing the magnetic mineral concentration in the sediments. Monsoon rain was found to act as a main agent in the process of transport of mine-waste to the Mandovi and Zuari estuaries ((Nayak, 1998 and references therein) which transport sediments to offshore Goa.

The combination of  $^{210}\text{Pb}$  dating and magnetic analyses allowed us to reliably determine the onset of mining induced changes in sedimentation and thereby differentiate the time periods of varying natural and anthropogenic influences. A sharp increase of these parameters in the Unit 1 indicates the increasing anthropogenic effects due to mining. Comparatively low values of concentration parameters  $\chi_{\text{LF}}$ , SIRM,  $\chi_{\text{ARM}}$  in the Unit 2 provides information about the background magnetic signal and to assess the post depositional alteration if any.

## **Influence of diagenesis on the magnetic minerals**

The variations in the mineral magnetic concentration parameters in the Unit 2 in this core are mainly related to the natural sedimentary processes but may also be affected by post depositional processes. Changes in the sediment source, particle size and post-depositional diagenesis can influence the magnetic properties of sediments (Dong et al., 2014). For assessing the sediment source changes, a discrimination diagram of La-Th-Sc (e.g., Nath et al., 2000) was used (**Fig. 9**). All these three elements are not affected by changes in magnetic mineralogy. Data of sediments from both the units overlap and have a similar spread which indicates that the sediment source and the composition remained same throughout the depositional period. Diagenetic alteration of iron oxides is possible due to changes in redox conditions in the bottom water and within the sediments which can also drive the deposition and decomposition of organic matter (Henshaw and Merrill, 1980; Karlin and Levi, 1983). These post depositional changes alter the existing magnetic mineral assemblages by the dissolution of existing minerals and the formation of new minerals and degrade or reprint the detrital magnetic signatures carried by them (Wheeler et al., 1999). Many studies have documented magnetic mineral diagenesis in the organic-rich sediments from the Arabian Sea (Bloemendal et al., 1993, 1992; Hounslow and Maher, 1999).

The rapid decrease in magnetic mineral concentration parameters in the 54 – 83 cm section (corresponding to 1908 – 1755 AD) in Unit 2 suggests the possible influence of early diagenesis in this depth (**Fig: 3**). The post depositional degradation of the organic matter rich sediments (average  $C_{org}$  concentration in this core = 2.61%, which is relatively high) causes the dissolution of detrital ferrimagnetic minerals and formation of iron sulphides (gregite, pyrite, mackinawite etc) in sulphidic environments (Rowan et al., 2009). The high surface area to volume ratio causes fine magnetic grains to dissolve earlier than coarse grains during early diagenesis (Yamazaki et al., 2014). Coarsening of magnetic grain size and the change in magnetic mineralogy at this subsurface depth (54 – 83 cm) may be due to early diagenesis. The coarsening of magnetic grain size is manifested by the  $\chi_{ARM} / \chi_{LF}$  and  $\chi_{ARM}/SIRM$  ratios (**Fig: 3**) and the plot of  $\chi_{ARM}/SIRM$  vs  $\chi_{FD}\%$  (**Fig: 4**) and indicate that fine grained ferrimagnetic minerals are selectively dissolved in this section (See Bloemendal et al., 1992; Karlin and Levi, 1983). The low value of S – ratio in this period marks an increase in concentration of antiferromagnetic minerals like hematite and a decrease in the concentration of soft magnetic minerals like magnetite. The high values of  $\chi_{LF}$  and the low concentration of  $C_{org}$  below 83 cm (**Fig: 10**) indicate the reduced influence of early diagenesis and can be treated as the ‘natural magnetic background signal’. In addition to the diagenetic changes, climatic influence is also visible in the lower part of the core. The down core variation of  $\chi_{LF}$  with

the total solar irradiance data (Lean et al., 1995),  $C_{org}$  and  $CaCO_3$  concentrations reveal that the core records the small-amplitude Holocene climate events Dalton minimum (~ 1790 – 1830 AD) and Maunder minimum (~ 1645 – 1715 AD) during the Little Ice Age (LIA) (**Fig: 10**). The Dalton minimum is marked in this core by an increase in Fe and Mn and a decrease in  $C_{org}$  concentration (**Fig: 10**). The reduction in  $C_{org}$  concentration indicates a decrease in the productivity during this period which may be due to the drastic reduction in the summer monsoon strength during the solar minima of Little Ice Age (Agnihotri et al., 2002; Gupta et al., 2013; Kurian et al., 2009).

## **Conclusions**

The mineral magnetic properties and geochemical studies of a dated sediment core from the inner continental shelf off Goa, west coast of India provide a clear record of historical changes in terrestrial mining induced sedimentation in the area. This study has enabled us to reconstruct the sedimentation history of the last three centuries and to understand the impact of iron ore mining in Goa on the offshore sedimentation. The results indicate that the sharp increase in the sedimentation rate along with an increase in mineral magnetic parameters at a depth of 41 cm corresponding to an age of 1982AD is a result of the increased iron ore mining activities in Goa. The rock magnetic record also reveals that the iron ore mining related sedimentation off Goa has intensified in 1970's, even though the mining in Goa has commenced at the beginning of 20<sup>th</sup> century. A close correspondence of increasing susceptibility values with the increased iron-ore production is noticed. The natural background magnetic signal was different from the mining-induced sediments which allowed us to understand the intensity of mining induced changes in the sediment history.

The rapid reduction of mineral magnetic concentration parameters along with an increase in the mineral magnetic grain size in 54 – 83 cm (subsurface) depth reveals that fine grained magnetites are selectively dissolved in this unit due to the early diagenesis as a result of redox changes and organic matter decomposition. Mineral magnetic and geochemical changes were found to correlate with periods of the Dalton and Maunder minima of Little Ice Age (LIA). Our study proves that the open cast iron ore mining in the state of Goa, India is affecting the sedimentation in the offshore region and may be detrimental to the oceanic environment. This study also indicates that environmental magnetic properties of coastal sediments can reflect the land use changes in the source areas.

## **Acknowledgements**

Authors are thankful to the Director, NIO, Goa, for his encouragement and support. Drs Parthiban, Prakash Babu, Pratima Kessarkar and Pawan Dewangan are gratefully acknowledged for their help during analyses and interpretation. Miss. Asha Upaskar and Prajith A are thanked for their help in

environmental magnetic measurements. We thank Mr. Anthony D'Souza, Ship Cell for helping us collect the sediment core used in this study. TS is thankful to CSIR - Shyama Prasad Mukherjee Fellowship (SPMF) for providing the research fellowship. This work is a contribution to CSIR XII Plan GEOSINKS (PSC0106) project. This is NIO's contribution No XXXX.

## References

Agnihotri, R., Dutta, K., Bhushan, R., Somayajulu, B.L., 2002. Evidence for solar forcing on the Indian monsoon during the last millennium. *Earth Planet. Sci. Lett.* 198, 521–527. doi:10.1016/S0012-821X(02)00530-7

Alagarsamy, R., 2006. Distribution and seasonal variation of trace metals in surface sediments of the Mandovi estuary, west coast of India. *Estuar. Coast. Shelf Sci.* 67, 333–339. doi:10.1016/j.ecss.2005.11.023

Bhala, U., Basavaiah, N., Deenadayalan, K., Borole, D. V, Mohite, R.D., 2011. Onset of industrial pollution recorded in Mumbai mudflat sediments, using integrated magnetic, chemical, <sup>210</sup>Pb dating, and microscopic methods. *Environ. Sci. Technol.* 45, 686–92. doi:10.1021/es1025905

Bloemendal, J., King, J.W., Hall, F.R., Doh, S.-J., 1992. Rock magnetism of Late Neogene and Pleistocene deep-sea sediments: Relationship to sediment source, diagenetic processes, and sediment lithology. *J. Geophys. Res.* 97, 4361. doi:10.1029/91JB03068

Bloemendal, J., King, J.W., Hunt, A., Demenocal, P.B., Hayashida, A., 1993. Origin of the sedimentary magnetic record at Ocean Drilling Program Sites on the Owen Ridge, western Arabian Sea. *J. Geophys. Res.* 98, 4199. doi:10.1029/92JB02914

Dearing, J.A., Bird, P.M., Dann, R.J.L., Benjamin, S.F., 1997. Secondary ferrimagnetic minerals in Welsh soils: a comparison of mineral magnetic detection methods and implications for mineral formation. *Geophys. J. Int.* 130, 727–736. doi:10.1111/j.1365-246X.1997.tb01867.x

Dekkers, M.J., 2007. Magnetic proxy parameters, in: Gubbins, D., Herrero-Bervera, E. (Eds.), *Encyclopedia of Geomagnetism and Palaeomagnetism*. Springer, pp. 525–534.

Dong, C., Zhang, W., Ma, H., Feng, H., Lu, H., Dong, Y., Yu, L., 2014. A magnetic record of heavy metal pollution in the Yangtze River subaqueous delta. *Sci. Total Environ.* 476–477, 368–377. doi:10.1016/j.scitotenv.2014.01.020

Fernandes, L., Nayak, G.N., 2009. Distribution of Sediment Parameters and Depositional Environment of Mudflats of Mandovi Estuary, Goa, India. *J. Coast. Res.* 252, 273–284. doi:10.2112/05-0614.1

Flynn, W.W., 1968. The determination of low levels of polonium-210 in environmental materials. *Anal. Chim. Acta* 43, 221–227. doi:10.1016/S0003-2670(00)89210-7

Gokul, A.R., Srinivasan, M. D., Gopalakrishnan, K., Vishwanathan, L., 1985. Stratigraphy and structure of Goa, in: *Proc. Sem. Earth Resources for Goa's Development*, Geol. Surv. India. p. 1–13.

Gupta, A.K., Mohan, K., Das, M., Singh, R.K., 2013. Solar forcing of the Indian summer monsoon variability during the Ållerød period. *Sci. Rep.* 3, 2753. doi:10.1038/srep02753

Henshaw, P.C., Merrill, R.T., 1980. Magnetic and chemical changes in marine sediments. *Rev. Geophys.* 18, 483. doi:10.1029/RG018i002p00483

Hounslow, M.W., Maher, B. a., 1999. Source of the climate signal recorded by magnetic susceptibility variations in Indian Ocean sediments. *J. Geophys. Res.* 104, 5047. doi:10.1029/1998JB900085

Jackson, M.L., 1958. *Soil chemical analysis*, Zeitschrift für Pflanzenernährung, Düngung, Bodenkunde. Prentice Hall, Inc., Englewood Cliffs, NJ. doi:10.1002/jpln.19590850311

Karlin, R., Levi, S., 1983. Diagenesis of magnetic minerals in Recent haemipelagic sediments. *Nature* 303, 327–330. doi:10.1038/303327a0

Kessarkar, P.M., Suja, S., Sudheesh, V., Srivastava, S., Rao, V.P., 2015. Iron ore pollution in Mandovi and Zuari estuarine sediments and its fate after mining ban. *Environ. Monit. Assess.* 187, 572. doi:10.1007/s10661-015-4784-z

King, J., Banerjee, S.K., Marvin, J., Özdemir, Ö., 1982. A comparison of different magnetic methods for determining the relative grain size of magnetite in natural materials: Some results from lake sediments. *Earth Planet. Sci. Lett.* 59, 404–419. doi:10.1016/0012-821X(82)90142-X

Koide, M., Soutar, A., Goldberg, E.D., 1972. Marine geochronology with <sup>210</sup>Pb. *Earth Planet. Sci. Lett.* 14, 442–446. doi:10.1016/0012-821X(72)90146-X

Krishnaswami, S., Lal, D., 1978. Radionuclide Limnology, in: Lerman, A. (Ed.), *Lakes: Chemistry, Geology, Physics*. Springer New York, New York, NY, pp. 153–177. doi:10.1007/978-1-4757-1152-3

Kurian, S., Agnihotri, R., Borole, D. V, Naqvi, S.W.A., Ferreira, A.N.A.M., Vale, C., 2009. Possible solar control on primary production along the Indian west coast on decadal to centennial timescale. *J. Quat. Sci.* 24, 109–116. doi:10.1002/jqs

Lean, J., Beer, J., Bradley, R., 1995. Reconstruction of solar irradiance since 1610: Implications for climate change. *Geophys. Res. Lett.* 22, 3195–3198. doi:10.1029/95GL03093

Maher, B. a., 1998. Magnetic properties of modern soils and Quaternary loessic paleosols: paleoclimatic implications. *Palaeogeogr. Palaeoclimatol. Palaeoecol.* 137, 25–54. doi:10.1016/S0031-0182(97)00103-X

Mesquita, A.M., Kaisary, S., 2007. Distribution of iron and manganese, in: Shetye, S.R., DileepKumar, M., Shankar, D. (Eds.), *The Mandovi and Zuari Estuaries*. National Institute of Oceanography, Goa, India.

Moskowitz, B.M., 1991. Hitchhiker ' s Guide to Magnetism, in: *Environmental Magnetism Workshop (IRM)*. Inst. for Rock Magnetism, Univ. of Minn., Minneapolis, Minn, p. 48.

Mullins, C.E., Tite, M.S., 1973. Magnetic viscosity, quadrature susceptibility, and frequency dependence of susceptibility in single-domain assemblies of magnetite and maghemite. *J. Geophys. Res.* 78, 804–809. doi:10.1029/JB078i005p00804

Nath, B.N., Kunzendorf, H., Pluger, W.L., 2000. Influence of Provenance, Weathering, and Sedimentary Processes on the Elemental Ratios of the Fine-Grained Fraction of the Bedload

Sediments from the Vembanad Lake and the Adjoining Continental Shelf, Southwest Coast of India. *J. Sediment. Res.* 70, 1081–1094. doi:10.1306/100899701081

Nayak, G.N., 1998. Impact of Mining on Environment in Goa: a review. *Environ. Geochemistry* 1, 97–100.

Nayak, G.N., 2002. Impact of mining on environment in Goa. India International Publishers, New Delhi.

Nigam, R., Panchang, R., Banerjee, P., 2005. Foraminifera in Surface Sediments of Mandovi River Estuary: Indicators for Mining Pollution and High Sea Stand in Goa, India. *J. Coast. Res.* 214, 853–859. doi:10.2112/03-0061.1

Oldfield, F., 1991. Environmental magnetism — A personal perspective. *Quat. Sci. Rev.* 10, 73–85. doi:10.1016/0277-3791(91)90031-O

Oldfield, F., Appleby, P.G., Van der Post, K.D., 1999. Problems of core correlation, sediment source ascription and yield estimation in Ponsonby Tarn, West Cumbria, UK. *Earth Surf. Process. Landforms* 24, 975–992. doi:10.1002/(SICI)1096-9837(199910)24:11<975::AID-ESP23>3.0.CO;2-W

Panchang, R., Nigam, R., Baig, N., Nayak, G.N., 2005. A foraminiferal testimony for the reduced adverse effects of mining in Zuari Estuary, Goa. *Int. J. Environ. Stud.* 62, 579–591. doi:10.1080/00207230500241801

Pascual, L.X., Pablos Cascallar, M., Planell i Calle, M., Puigdollers Rodés, E., Solé Carbonell, C., Vila i Casau, A., Martínez Alier, J., 2013. Iron mining in Goa (India) : an interdisciplinary study.

Prajith, A., Rao, V.P., Kessarkar, P.M., 2015. Magnetic properties of sediments in cores from the Mandovi estuary, western India: Inferences on provenance and pollution. *Mar. Pollut. Bull.* 99, 338–45. doi:10.1016/j.marpolbul.2015.07.034

Rowan, C.J., Roberts, A.P., Broadbent, T., 2009. Reductive diagenesis, magnetite dissolution, greigite growth and paleomagnetic smoothing in marine sediments: A new view. *Earth Planet. Sci. Lett.* 277, 223–235. doi:10.1016/j.epsl.2008.10.016

Shynu, R., Purnachandra Rao, V., Kessarkar, P.M., Rao, T.G., 2012. Temporal and spatial variability of trace metals in suspended matter of the Mandovi estuary, central west coast of India. *Environ. Earth Sci.* 65, 725–739. doi:10.1007/s12665-011-1119-4

Shynu, R., Rao, V.P., Kessarkar, P.M., Rao, T.G., 2011. Rare earth elements in suspended and bottom sediments of the Mandovi estuary, central west coast of India: Influence of mining. *Estuar. Coast. Shelf Sci.* 94, 355–368. doi:10.1016/j.ecss.2011.07.013

Shynu, R., Rao, V.P., Parthiban, G., Balakrishnan, S., Narvekar, T., Kessarkar, P.M., 2013. REE in suspended particulate matter and sediment of the Zuari estuary and adjacent shelf, western India: Influence of mining and estuarine turbidity. *Mar. Geol.* 346, 326–342. doi:10.1016/j.margeo.2013.10.004

Singh, K.T., 2007. Sedimentology and geochemistry of tidal mudflats along central west coast of India. Goa University.

Singh, K.T., Nayak, G.N., Fernandes, L.L., Borole, D.V., Basavaiah, N., 2014. Changing environmental conditions in recent past — Reading through the study of geochemical characteristics, magnetic parameters and sedimentation rate of mudflats, central west coast of India. *Palaeogeogr. Palaeoclimatol. Palaeoecol.* 397, 61–74. doi:10.1016/j.palaeo.2013.04.008

Thompson, R., Oldfield, F., 1986. *Environmental Magnetism*. Springer Netherlands, Dordrecht. doi:10.1007/978-94-011-8036-8

Veerasingam, S., Vethamony, P., Mani Murali, R., Fernandes, B., 2015. Depositional record of trace metals and degree of contamination in core sediments from the Mandovi estuarine mangrove ecosystem, west coast of India. *Mar. Pollut. Bull.* 91, 362–7. doi:10.1016/j.marpolbul.2014.11.045

Walden, J., 1999. Remanence measurements, in: Walden, J., Oldfield, F., Smith, J. (Eds.), *Environmental Magnetism: A Practical Guide*. Quaternary Research Association, London, p. 63–87.

Walkley, A., 1947. A critical examination of a rapid method for determining organic carbon in soils - Effect of variations in digestion conditions and of inorganic soil constituents. *Soil Sci.* 63, 251–264. doi:10.1097/00010694-194704000-00001

Wheeler, A.J., Oldfield, F., Orford, J.D., 1999. Depositional and post-depositional controls on magnetic signals from saltmarshes on the north-west coast of Ireland. *Sedimentology* 46, 545–558. doi:10.1046/j.1365-3091.1999.00236.x

Yamazaki, T., Abdeldayem, A.L., Ikehara, K., 2014. Rock-magnetic changes with reduction diagenesis in Japan Sea sediments and preservation of geomagnetic secular variation in inclination during the last 30,000 years. *Earth, Planets Sp.* 55, 327–340. doi:10.1186/BF03351766

Yu, L., Oldfield, F., 1993. Quantitative sediment source ascription using magnetic measurements in a reservoir-catchment system near Nijar, S.E. Spain. *Earth Surf. Process. Landforms* 18, 441–454. doi:10.1002/esp.3290180506

Zingde, M.D., Singbal, S.Y.S., Moraes, C.F., Reddy, C.V.G., 1976. Arsenic, Copper, Zinc & Manganese in the Marine Flora & Fauna of Coastal & Estuarine Waters around Goa. *Indian J. Mar. Sci.* 5, 212–217.

<http://www.cseindia.org/node/386>, Mining in Goa, Centre for science and environment, Accessed on 09/05/2016

[www.goadmg.gov.in/MiningArea.aspx](http://www.goadmg.gov.in/MiningArea.aspx), Mining Area, Directorate of Mines & Geology, Government of Goa

## Description of figures and tables

**Figure 1:** Map showing the mining areas in Goa, India (Shaded Red) along with the rivers and major cities (Modified from [http://cseindia.org/mining/1district\\_goa.htm](http://cseindia.org/mining/1district_goa.htm)). The sampling location is also shown in the figure.

**Figure 2:** Figure showing the changes in sedimentation rate obtained from different studies around Goa using  $^{210}\text{Pb}$  dating technique. 1) Present study, 2) Singh et al, (2014), 3) Kurian et al (2009). The locations of these sediment cores are shown in the figure for comparison.

**Figure 3:** Down core variation in linear sedimentation rate,  $\text{CaCO}_3$ ,  $\text{C}_{\text{org}}$  and environmental magnetic parameters (of concentration, grain size and mineralogy of the magnetic minerals) indicating a clear difference between two units.

**Figure 4:** A figure of  $\chi_{\text{fd}}\%$  versus  $\chi_{\text{ARM}}/\text{SIRM}$  ratio indicates a distinct change in magnetic grain size and the concentration of super paramagnetic (SP) grains in two units.

**Figure 5:** Comparison between the mineral magnetic properties obtained from this study from the inner shelf off Goa (Black) with the study from Mandovi mudflat region (Singh et al., 2014) (Red).

**Figure 6:** Comparison between the magnetic susceptibility and iron ore production (decadal scale) in Goa (Production data from Nayak, 2002; Pascual et al., 2013)

**Figure 7:** Scatter plots between a)  $\chi_{\text{LF}}$  vs Fe, b)  $\chi_{\text{LF}}$  vs S - ratio, c)  $\chi_{\text{ARM}}$  vs  $\chi_{\text{LF}}$  and d)  $\chi_{\text{ARM}}/\text{SIRM}$  vs  $\chi_{\text{LF}}$  showing a distinct zonation between the pre-mining and post-mining period.

**Figure 8:** Figure showing the relationship between Konkan – Goa rainfall and the magnetic susceptibility during the years 1980 – 2007.

**Figure 9:** La–Th–Sc ternary diagram showing the provenance characteristics of the sediments. All the points fall closely indicating that the provenance has remained same throughout the time period the core has covered.

**Figure 10:** Graph showing the variation of  $\chi_{\text{LF}}$  with Fe, Mn,  $\text{C}_{\text{org}}$  and  $\text{CaCO}_3$  and Total Solar Irradiance (TSI) concentrations. The shaded region in the top indicates the anthropogenically influenced zone while the shaded region in the middle indicates the influence of early diagenesis.

**Table 1:** Comparison between major mineral magnetic parameters obtained from different studies in the Mandovi – Zuari estuaries and the offshore region. (\* from (Singh, 2007) - Fe concentrations not given separately for each section by the author.)



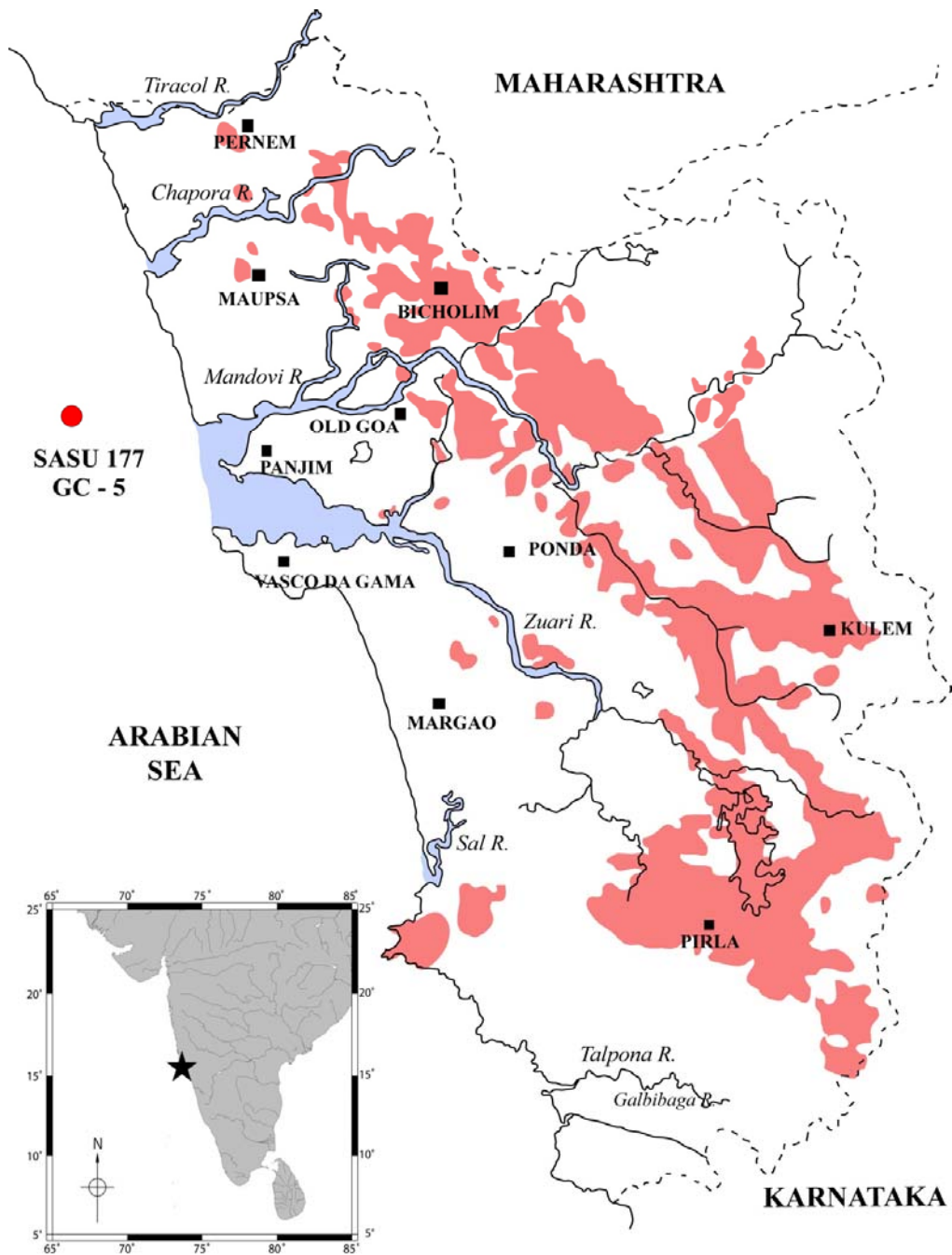


**Figure 1:** Map showing the mining areas in Goa, India (Shaded Red) along with the rivers and major cities (Modified from [http://cseindia.org/mining/1district\\_goa.htm](http://cseindia.org/mining/1district_goa.htm)). The sampling location is also shown in the figure.

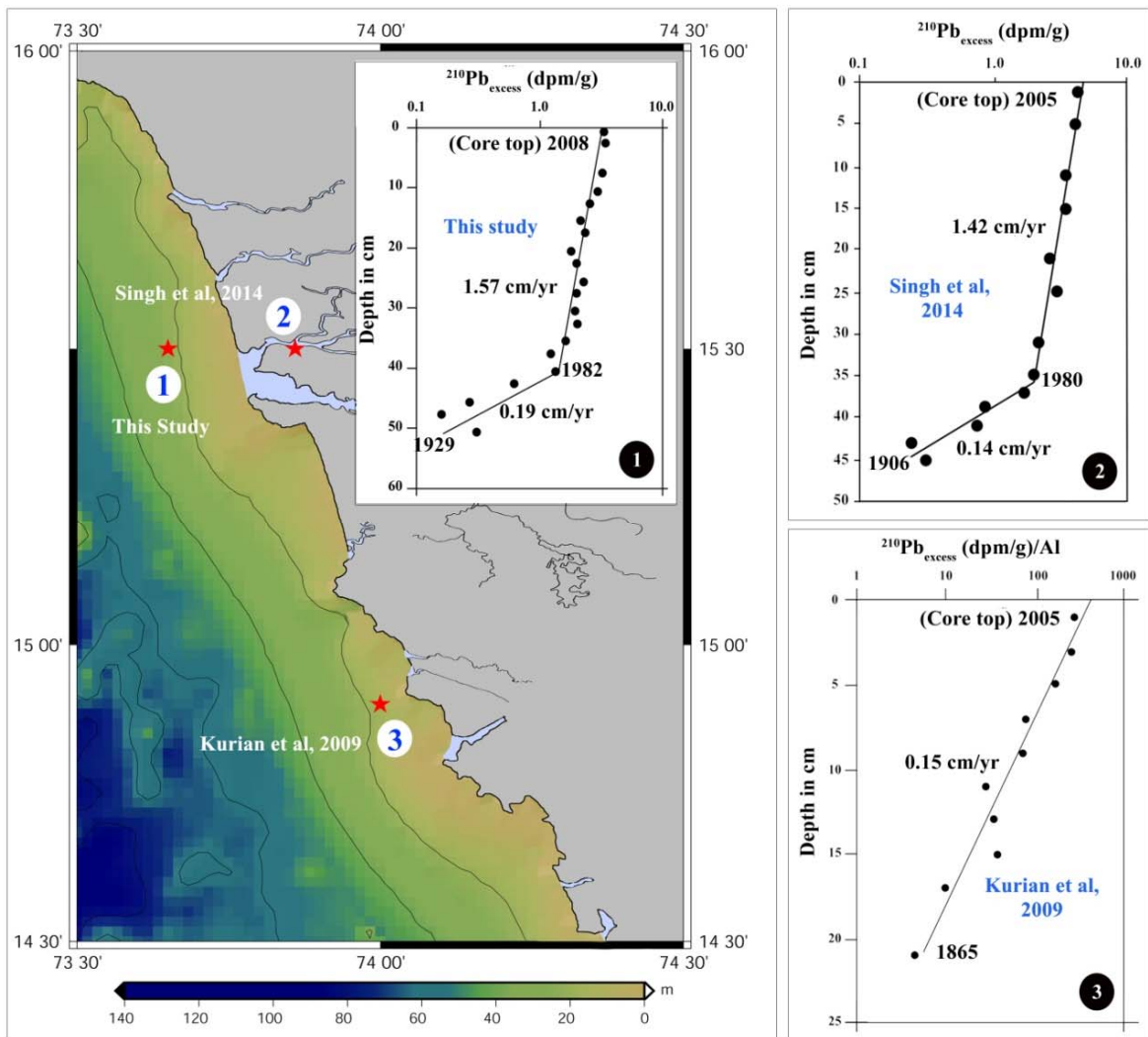


**Figure 2:** Figure showing the changes in sedimentation rate obtained from different studies around Goa using  $^{210}\text{Pb}$  dating technique. 1) Present study, 2) Singh et al, (2014), 3) Kurian et al (2009). The locations of these sediment cores are shown in the figure for comparison.

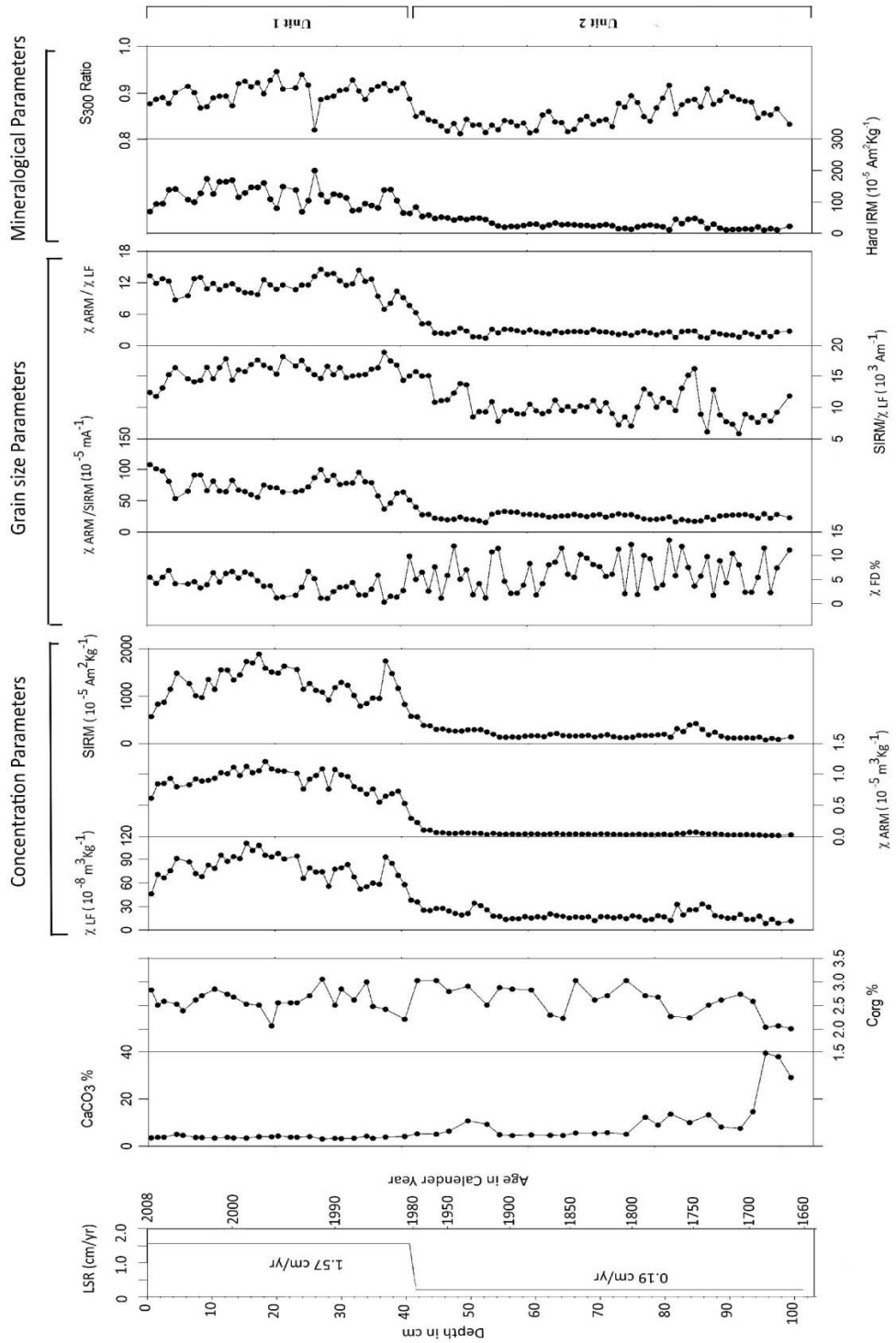


**Figure 3:** Down core variation in linear sedimentation rate, CaCO<sub>3</sub>, C<sub>org</sub> and environmental magnetic parameters (of concentration, grain size and mineralogy of the magnetic minerals) indicating a clear difference between two units.

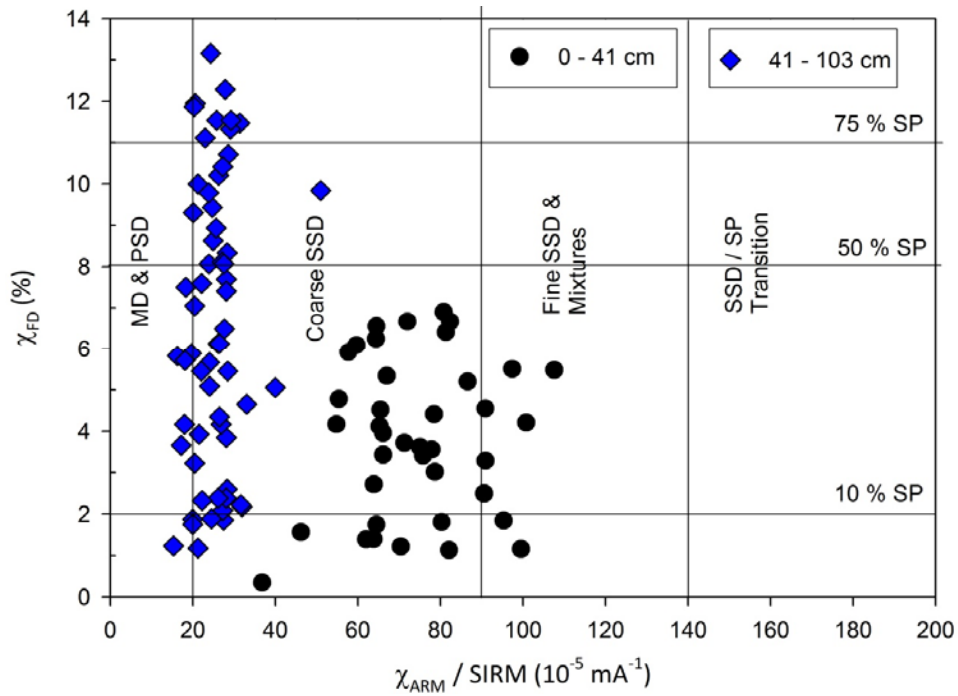


**Figure 4:** A figure of  $\chi_{fd}\%$  versus  $\chi_{ARM}/SIRM$  ratio indicates a distinct change in magnetic grain size and the concentration of super paramagnetic (SP) grains in two units.

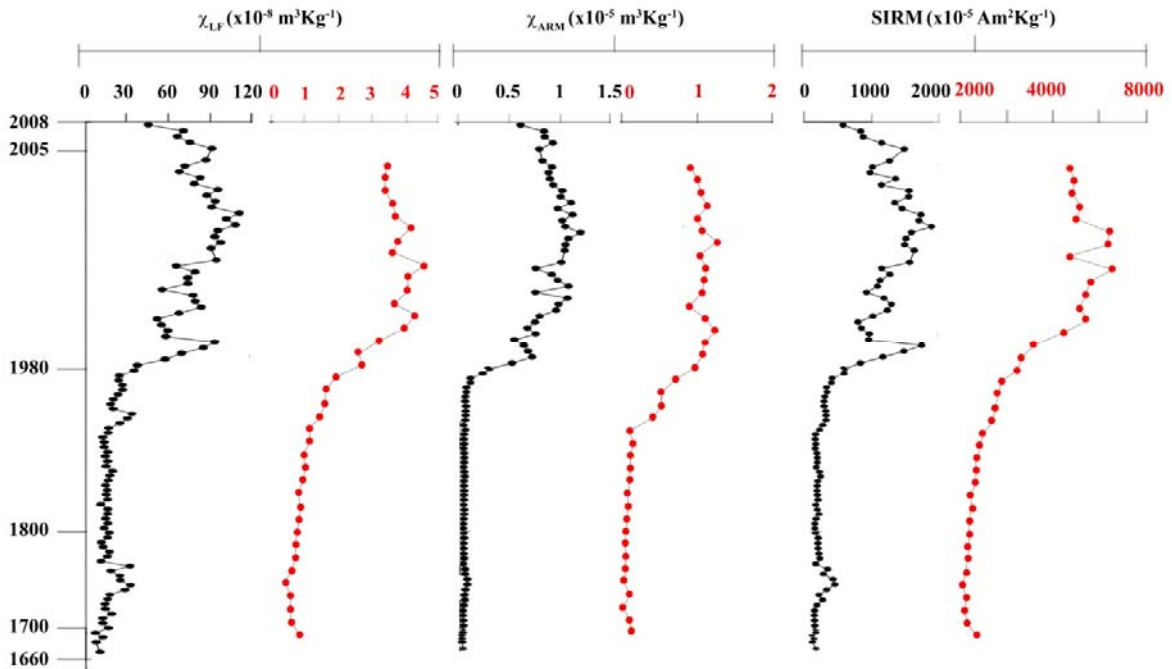


**Figure 5:** Comparison between the mineral magnetic properties obtained from this study from the inner shelf off Goa (Black) with the study from Mandovi mudflat region (Singh et al., 2014) (Red).

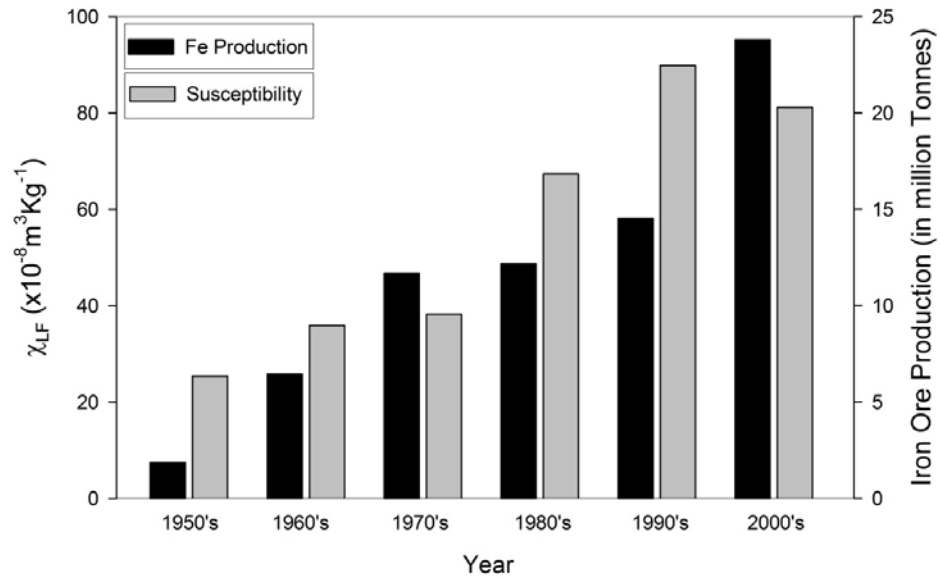


**Figure 6:** Comparison between the magnetic susceptibility and iron ore production (decadal scale) in Goa (Production data from Nayak, 2002; Pascual et al., 2013).

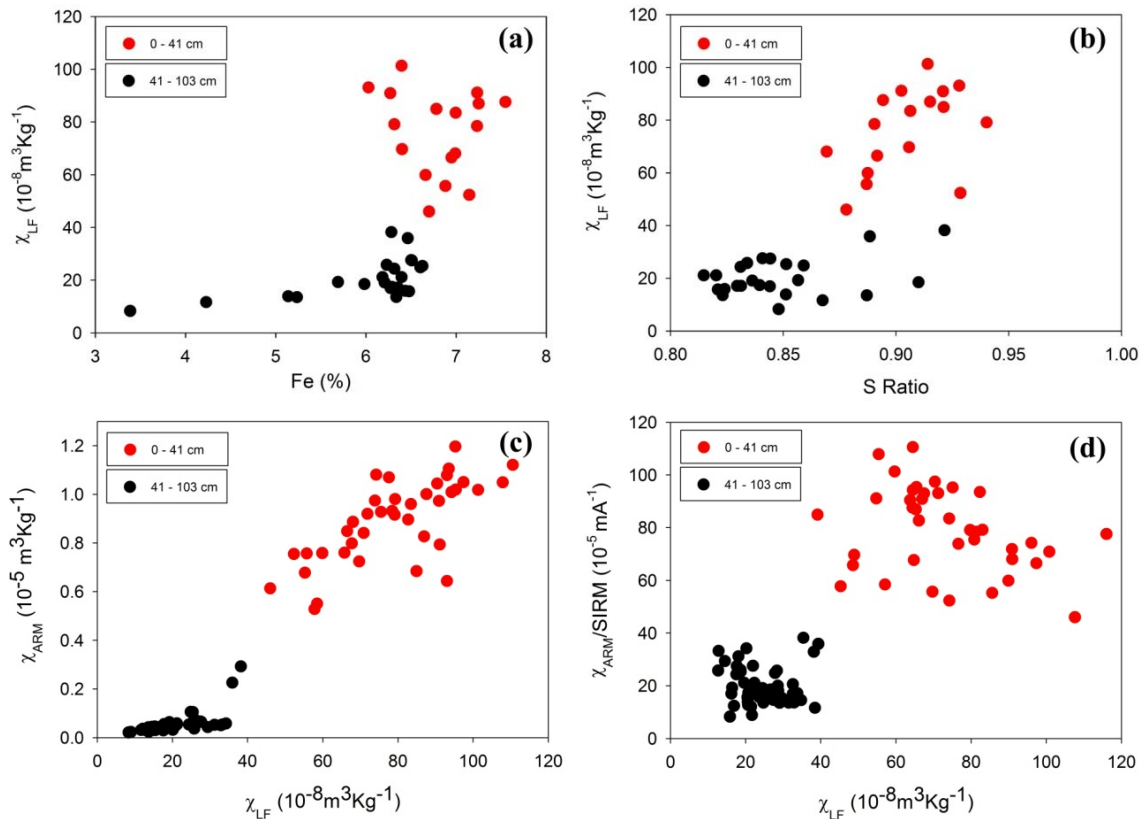


**Figure 7:** Scatter plots between a)  $\chi_{LF}$  vs Fe, b)  $\chi_{LF}$  vs S Ratio, c)  $\chi_{ARM}$  vs  $\chi_{LF}$  and d)  $\chi_{ARM}/SIRM$  vs  $\chi_{LF}$  showing a distinct zonation between the pre-mining and post-mining period.

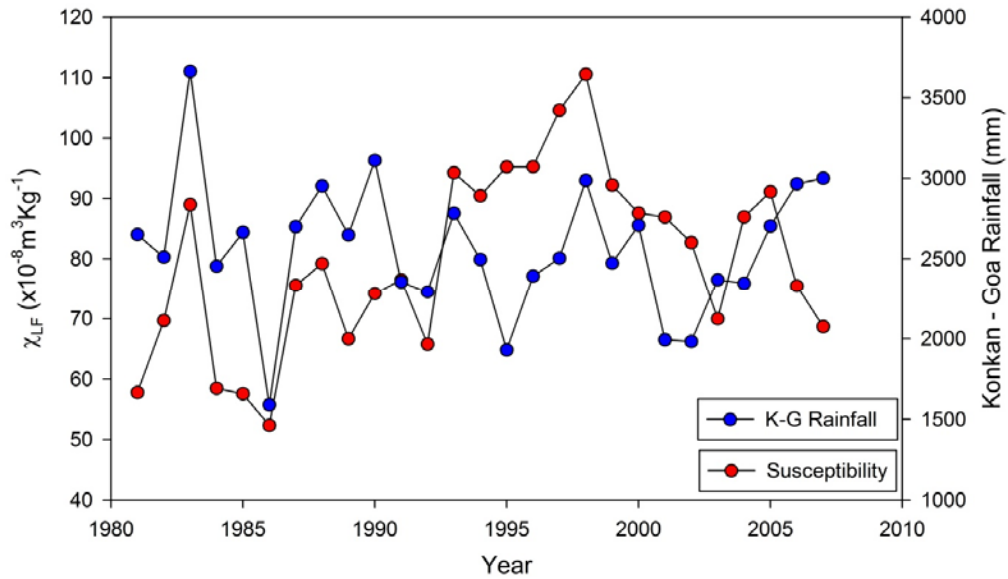


**Figure 8:** Figure showing the relationship between Konkan – Goa rainfall and the magnetic susceptibility during the years 1980 – 2007.

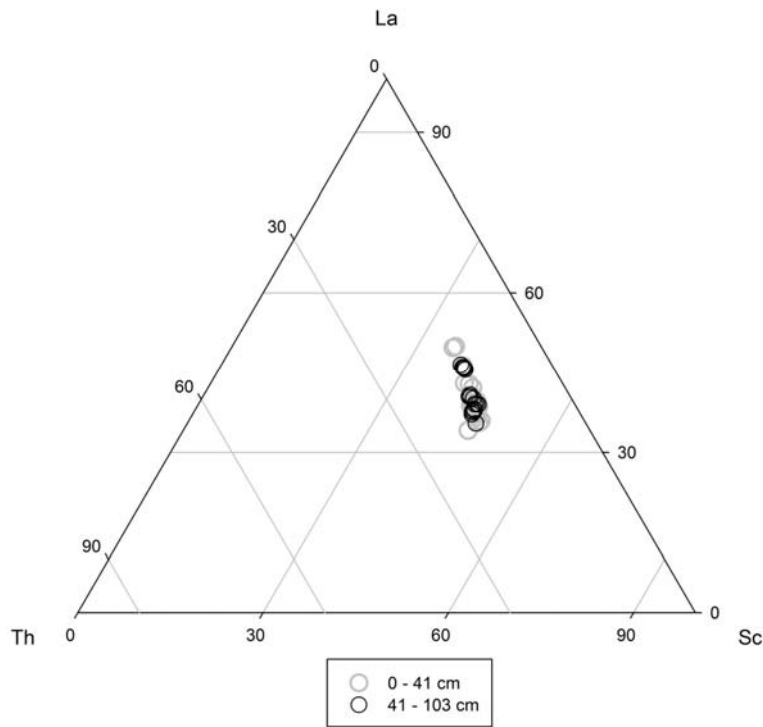


**Figure 9:** La–Th–Sc ternary diagram showing the provenance characteristics of the sediments. All the points fall closely indicating that the provenance has remained same throughout the time period the core has covered.

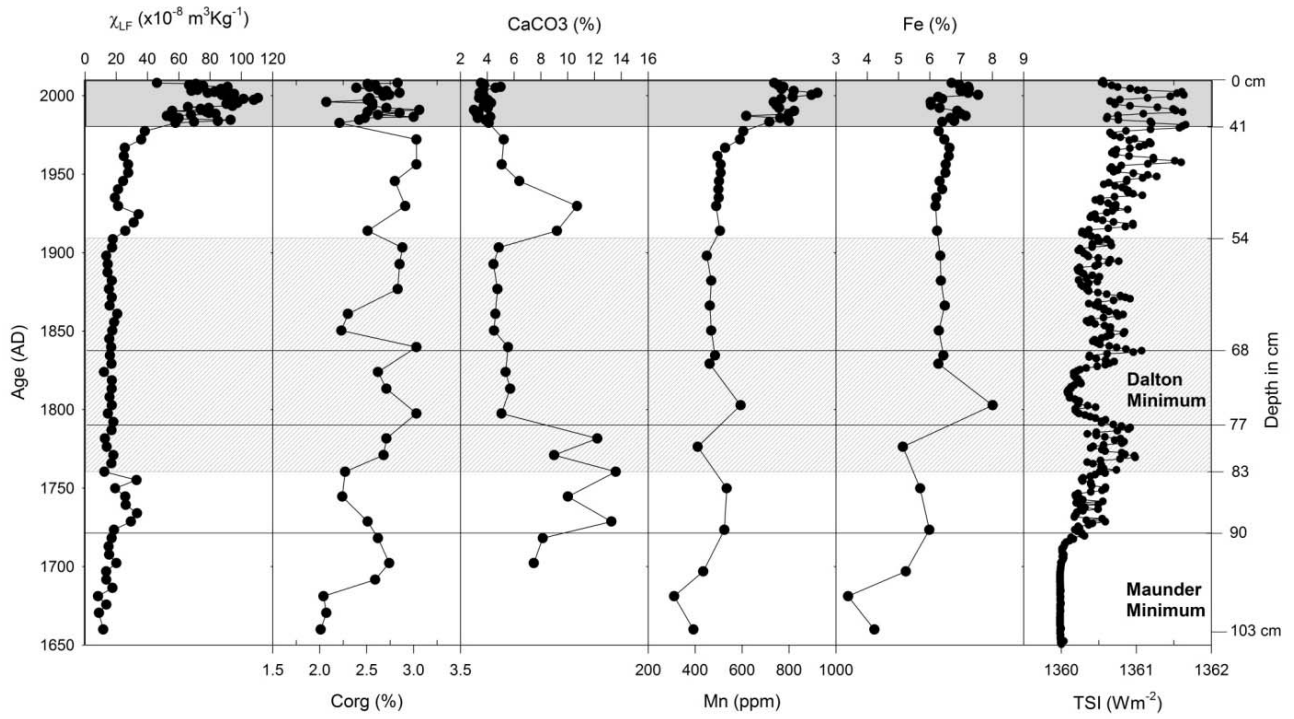


**Figure 10:** Graph showing the variation of  $\chi_{LF}$  with Fe, Mn, C<sub>org</sub> and CaCO<sub>3</sub> and Total Solar Irradiance (TSI) concentrations. The shaded region in the top indicates the anthropogenically influenced zone while the shaded region in the middle indicates the influence of early diagenesis.

**Table 1:** Comparison between major mineral magnetic parameters obtained from different studies in the Mandovi – Zuari estuaries and the offshore region. (\* from (Singh, 2007) - Fe concentrations not given separately for each section by the author.)

	Sediment core from the shelf off Mandovi-Zuari estuaries (This study)		Surface samples from the shelf off Mandovi-Zuari estuaries (Kessarkar et al, 2015)	Sediment core from the mudflat region of Mandovi River (Singh et al, 2014)			Sediment cores from the Mandovi estuary. (Prajith et al, 2015)	
	0 - 41 cm	42 - 103 cm		0 - 30 cm	31 - 50 cm	51 - 76 cm	Lower estuary	Aguda Bay
$\chi_{LF}$ ( $10^{-8}$ m <sup>3</sup> kg <sup>-1</sup> )	79.1	19.4	79.3	3.493 ± 0.381	1.329 ± 0.613	0.423 ± 0.141	121.7	154.7
$\chi_{ARM}$ ( $10^{-5}$ m <sup>3</sup> kg <sup>-1</sup> )	0.89	0.05	0.6522	1.08 ± 0.10	0.48 ± 0.36	0.08 ± 0.03	0.9	0.6
$\chi_{FD}$	3.9	6.6	3.9	3.67 ± 0.57	1.84 ± 1.65	0.93 ± 0.87	4.5	7.6
SIRM ( $10^{-5}$ Am <sup>2</sup> kg <sup>-1</sup> )	1249.6	205.8	11262.0	5193 ± 850	1453 ± 704	391 ± 164	1450	2240
SIRM/ $\chi_{LF}$ ( $10^3$ Am <sup>-1</sup> )	16.1	10.9	14.7	—	—	—	12.3	14.5
$\chi_{ARM}/\chi_{LF}$	11.4	2.6	13.8	0.3 ± 0.04	0.3 ± 0.1	0.2 ± 0.1	6.6	4.8
$\chi_{ARM}/SIRM$ ( $10^{-5}$ mA <sup>-1</sup> )	73.2	24.9	—	20	30	20	54.9	33.1
S Ratio	0.90	0.86	0.942	0.69 ± 0.04	0.86 ± 0.03	0.82 ± 0.07	0.928	0.898
Soft IRM	1028.2	163.1	—	3502 ± 438	1371 ± 659	344 ± 125	—	—
Hard IRM	119.3	29.8	—	1643 ± 379	216 ± 151	72 ± 61	—	—
Fe (%)	6.77	6.40	—		19.91 - 5.81*		5.4	7.2